




# Unraveling the temperature-dependent plastic deformation mechanisms of polycrystalline Ta implants through numerical analysis of grain boundary dynamics

A. Kardani<sup>1</sup>, A. Montazeri<sup>1,2</sup>, and H. M. Urbassek<sup>3,4,\*</sup> 

<sup>1</sup> Computational Nanomaterials Lab (CNL), Faculty of Materials Science and Engineering, K. N. Toosi University of Technology, Tehran, Iran

<sup>2</sup> School of Nano Science, Institute for Research in Fundamental Sciences (IPM), Tehran 19395-5531, Iran

<sup>3</sup> Physics Department, University Kaiserslautern, Erwin-Schrödinger-Straße, 67663 Kaiserslautern, Germany

<sup>4</sup> Research Center OPTIMAS, University Kaiserslautern, Erwin-Schrödinger-Straße, 67663 Kaiserslautern, Germany

Received: 17 April 2022

Accepted: 11 August 2022

Published online:

29 August 2022

© The Author(s) 2022

## ABSTRACT

Nanostructured tantalum (Ta)-based dental implants have recently attracted significant attention thanks to their superior biocompatibility and bioactivity as compared to their titanium-based counterparts. While the biological and chemical aspects of Ta implants have been widely studied, their mechanical features have been investigated more rarely. Additionally, the mechanical behavior of these implants and, more importantly, their plastic deformation mechanisms are still not fully understood. Accordingly, in the current research, molecular dynamics simulation as a powerful tool for probing the atomic-scale phenomena is utilized to explore the microstructural evolution of pure polycrystalline Ta samples under tensile loading conditions. Various samples with an average grain size of 2–10 nm are systematically examined using various crystal structure analysis tools to determine the underlying deformation mechanisms. The results reveal that for the samples with an average grain size larger than 8 nm, twinning and dislocation slip are the main sources of any plasticity induced within the sample. For finer-grained samples, the activity of grain boundaries—including grain elongation, rotation, migration, and sliding—are the most important mechanisms governing the plastic deformation. Finally, the temperature-dependent Hall–Petch breakdown is thoroughly examined for the nanocrystalline samples via identification of the grain boundary dynamics.

Handling Editor: P. Nash.

Address correspondence to E-mail: [urbassek@rhrk.uni-kl.de](mailto:urbassek@rhrk.uni-kl.de)

## Introduction

In recent years, implants have been recognized as one of the most common treatment options to replace decayed teeth. Using surgical methods, implants are placed into the jawbone providing the required strength for the installation of dental prostheses. It is worth mentioning that the success of this technique is highly dependent on the use of proper materials and a suitable mechanical design. The metal used in the implant body should be highly resistant to mechanical stresses, wear, and corrosion. Additionally, it must possess high biocompatibility without toxicity [1, 2]. Considering the enumerated features, so far, the majority of studies on dental implants have been devoted to titanium (Ti) alloys. Compared to the well-known Ti implants, their tantalum (Ta)-based counterparts offer multiple benefits associated with their higher corrosion and wear resistance, biocompatibility and bioactivity [3–6]. This metal also shows enhanced phase stability and closer mechanical properties to the jawbone. It should be noted that based on Wolff's law, modulus matching is needed to reduce the stress-shielding in the load-bearing metallic implants [7, 8]. Furthermore, based on the biological *in vitro* and *in vivo* studies, Ta implants have better osseointegration and cell adhesion, making them ideal for therapeutic purposes [9, 10]. Hence, Ta-based implants are expected to be focal research points in the near future. The major barrier to extending the use of tantalum implants is the possibility that bacterial adhesion to their surface might lead to implant-associated infections. To overcome this issue, in addition to pristine Ta, several experimental investigations have been carried out to examine the performance of their nanocomposite systems in surgical implant applications. In this context, previous studies have revealed that the addition of copper and silver to the Ta structure can considerably improve its antibacterial properties [11, 12]. It has been established that these two antibacterial agents can effectively destroy the bacterial cell wall preventing the inflammation after treatment.

A review of the current literature shows that while the biological and chemical aspects of Ta-based nanocomposite implants have been widely investigated in recent years, their mechanical features have rarely been studied. Considering the importance of

the mechanical characteristics of dental implants, a noticeable gap in this research area has been the lack of a computational model to explore the load-bearing features of tantalum implants in the presence of different antibacterial additives such as Cu and Ag. More importantly, the proposed implants should be designed such that no plastic deformation occurs under the service conditions [13, 14]. Since the latter is mainly influenced by the overall behavior of the matrix, it seems that as the first step, a thorough analysis should be performed to examine the strength of polycrystalline tantalum and its plastic deformation behavior. As discussed in the literature, the elasticity of polycrystalline metals considerably depends on the type of their crystalline structure and the density of grain boundaries (GBs) [15, 16]. Also, the slip of dislocations and twinning has been recognized as the main sources of plastic deformation within these nanostructured materials [17, 18]. It is worth mentioning that the mechanisms governing their plastic deformation deal with only a small number of atoms or atomic layers, which cannot be simply examined through experiment-based techniques. Moreover, there are several limitations on the precise control and measurement at the atomic scale. Hence, numerical tools such as molecular dynamics (MD) simulation would provide an efficient way to characterize the microstructural evolution of these materials at the atomic scale [19, 20].

As the present work aims to provide a comprehensive MD-based study on the mechanical features of polycrystalline Ta systems under different service conditions, we will look at the current trends in this research area. Utilizing this approach, the mechanical behavior of polycrystalline Ta under uniaxial tensile loading has been investigated by Pan et al. [21]. It is noted that in FCC metals, the nucleation of partial dislocations with concurrent formation of stacking faults between them leads to the formation of twins as the main cause of plastic deformation. In contrast, for nanocrystalline BCC Ta samples, the results [21] revealed that owing to the GB movement, the deformation twinning is observed within the grains. Additionally, it was shown that in BCC metals, twinning-based deformation is favored at higher strain rates and/or lower temperature conditions. Also, more recently, Sun et al. [22] conducted MD simulations of tensile deformation on the Ta nanolayered structures composed of alternating nanocrystalline and coarse-grained layers. The main

goal was to assess the governing deformation and fracture mechanism of BCC nanolayered composites. Their findings revealed that compared to the twin nucleation, twin thickening is the favored mechanism for these materials. It arises because the energy required for the thickening of the twin domains is lower than the formation energy of new twins. Simulating polycrystalline Ta samples with different grain sizes in the range of 2–10 nm, Huang et al. [23] found that the critical size at which the Hall–Petch relationship is broken—at the temperature of 10 K—is equal to 7 nm. It was deduced that the enhanced activity of GBs in the samples with a grain size smaller than the critical limit is the main factor affecting the observed softening behavior passing the introduced threshold value.

An important question that should arise at this point is whether test factors such as type of loading, strain rate, and temperature can have a remarkable effect on the breakdown of the Hall–Petch relationship or change the deformation mechanisms of this material. In this regard, Tang et al. [24] showed that polycrystalline Ta has a much softer behavior in compressive loading than for tension that was ascribed to the enhanced dislocation motion under compression. In addition, Smith et al. [25] demonstrated that no correlation exists between the GB sliding and strain rate in this case. However, previous studies on platinum [26] and magnesium [27] have reported that increasing the temperature can noticeably facilitate the plastic deformation of polycrystalline nanomaterials by activating the GB motion. Consequently, the critical grain size introduced in the Hall–Petch relationship could be changed with temperature. To the best of our knowledge, this issue has not been studied for polycrystalline Ta. Furthermore, it has been shown that GBs may act as a place for the nucleation of dislocations and/or for inhibiting their movement in nanocrystalline materials [21, 24]. On the other hand, GB sliding should be considered as a vital grain size sensitive mechanism underlying the deformation of these materials [28].

In the present paper, we employ a series of MD simulations to precisely determine the exact role of GBs on the microstructural evolution of Ta samples under uniaxial tensile loadings. Considering the unique biological properties of Ta-based implants, at first, the critical grain size of polycrystalline Ta resulting in the maximum strength is obtained for the temperature of the human body. Targeting this

purpose, the mechanical response of various samples with an average grain of 2–10 nm is examined. The results are supported by a thorough inspection of the governing mechanisms using several crystal structure analysis tools. Finally, to examine the effect of temperature as a practical laboratory factor on the plastic deformation of nanostructured materials, a systematic study is performed at a higher temperature of 600 K to atomistically monitor the temperature-dependent Hall–Petch evolutions for the introduced polycrystalline Ta samples.

## Molecular dynamics model

### Sample construction

This section is devoted to explaining the details of the simulation processes along with introducing the algorithm utilized for generating the computational models. For this purpose, first, the procedure used for the sample construction is briefly explained. All polycrystalline Ta samples were built based on the Voronoi tessellation technique, which has been successfully utilized for the generation of representative models of polycrystalline microstructures of metals and their alloys [29, 30]. According to this method, using random seeds, Ta grains in the average size ranges from 2 to 10 nm were grown in 9 cubic samples having the same edge length of 30 nm. As previously discussed, the main aim of this study was to examine the role of grain size on the stress–strain response of Ta. Since the mechanical properties of nanomaterials are also influenced by the sample size, by keeping fixed the geometrical features of the computational cell, we could properly address the grain-size-dependent mechanical characteristics of the introduced tantalum systems. Figure 1 represents the microstructure of Ta sample with an average grain size of 8 nm.

### Details of MD simulation

All simulations were carried out using LAMMPS [31], and the angular-dependent potential (ADP) was employed to model the interatomic interactions within the Ta samples. Pun et al. [32] were the first who introduced the ADP format as a modified version of the well-known embedded-atom-method (EAM) potential function to analyze the structural

stability and strength of polycrystalline Ta structures. It has been demonstrated that using the newly developed ADP potential for tantalum, more accurate outcomes regarding the microstructural changes of elemental Ta and its alloys can be achieved at a more reasonable computational cost [33–36]. Before starting any mechanical test, the samples should be in thermodynamical equilibrium. Performing relaxation via suitable equilibrium ensembles allows the samples to attain the equilibrated structure starting from their geometrically constructed initial model. Regarding this issue, we designed a hybrid relaxation scheme to guarantee the system equilibrium. First, a minimization step using the conjugate gradient method was applied to avoid any atomic overlapping. Then, relaxation was followed by an annealing process at the temperature of 310 K (i.e., body temperature) for 200 ps. Finally, to equilibrate the grain boundaries, the samples experienced a further high-temperature annealing at 1000 K for 200 ps. Detailed explanation about this extra relaxation stage can be found in Ref. [37]. The pressure was set at zero during the whole equilibration procedure in the three directions of X, Y, and Z using an isothermal-isobaric (NPT) ensemble. The initial velocities were randomly sampled from a Maxwell–Boltzmann distribution at the desired temperature, and the velocity-Verlet integration algorithm with a time-step of 1 fs was utilized to advance the system variables [38]. Also, periodic boundary conditions were applied in all directions.

Figure 2 compares the microstructural features of annealed Ta polycrystals with an average grain size of 10 nm with those of the initial model. As seen, all the straight GBs exhibit curved morphology after the annealing procedure, demonstrating that the equilibrated samples have a similar configuration to the real microstructures detected in the experimental observations [39]. We were also concerned about the grain growth during the prescribed annealing stage. As such, having in hand the average value of initial grain size ( $d_0$ ), the grain size after relaxation ( $d$ ) can be determined using the following relation introduced in detail in Ref. [32]:

$$d = d_0 X_0 / X \quad (1)$$

where  $X_0$  and  $X$  are the number of GB atoms in the initial sample and in the fully relaxed structure, respectively. Substituting the data provided by the

crystal structure analysis tools into Eq. (1), an average grain size of  $\sim 10.2$  nm was obtained, indicating no sign of any grain growth during the relaxation stage. In addition, for further assessment of the morphological changes of the tantalum sample after the equilibration process, we monitored the grain rotation based on the axis-angle grain orientation algorithm [40, 41]. As thoroughly discussed in Refs. [42–44], employing this approach, the mean orientation of each grain can be computed based on the local structural environment and orientation of atoms within the grain. As illustrated in Fig. 2, a minor grain rotation was observed during the proposed hybrid annealing process.

After verifying the equilibrium stage, uniaxial elongation was carried out for all samples along opposite sides of the simulation box with a strain rate of  $5 \times 10^8 \text{ s}^{-1}$  until the strain level of 40% [23, 45, 46]. It is worth noting that the stress components in the lateral directions were kept constant at zero using the NPT ensemble during the whole procedure.

### Crystal structure analysis tools

To visualize the microstructure of all samples, the OVITO software package was implemented [47]. To better display and characterize the microstructural changes, the polyhedral template matching (PTM) was utilized. This modifier provides a direct calculation of local (per-atom) crystal orientation, elastic deformation, and strain in the presence of strong thermal fluctuations [42]. Additionally, to identify the dislocations and to calculate the dislocation density within the systems, the dislocation extraction algorithm (DXA) developed by Stukowski and Albe was employed [48]. Also, the determination of the von Mises stress distribution helped us determine the stress concentration in the GBs and grain interiors. Moreover, concerning the crucial role of twin formation on the results and the underlying mechanisms, twinning boundaries were monitored by means of the Centro-Symmetry Parameter (CSP), which provides a measure for deviation of a typical atom from its symmetric crystal structure [49]. Finally, to probe the grain orientations at the desired strain level, we used the grain segmentation analysis tool in the OVITO software.



## Results and discussion

### Polycrystalline Ta samples under tension: mechanical properties

At the start of the results part, we are going to look at the validation test. For this purpose, a polycrystalline tantalum sample with an average grain size of 3 nm was analyzed under the developed tensile test, and the results were compared with the data reported by Huang et al. [23] performed with an EAM potential at 10 K. To facilitate a better comparison, most of our simulation parameters, including the loading rate, temperature, geometrical characteristics of the computational model, and the average grain size, were similar to those of Ref. [23]. As seen in Table 1, the results are in good agreement with the presented data verifying the developed code. The small differences between the results may be associated with the different potential functions and relaxation schemes implemented in these two works. Employing the verified tensile code, the next step involved analysis of the effect of grain size on the mechanical characteristics of the Ta samples introduced in Sect. 2.1. Figure 3 displays the corresponding stress–strain curves that can be utilized to determine the elastic modulus and the flow stress of the samples. In the present work, the elastic modulus was directly computed as the initial slope of the stress–strain curve in the elastic region (i.e.,  $\varepsilon < 2\%$ ). Additionally, the yield strength is defined as the stress level at which the first plastic deformations occurred within the samples. As seen in this figure, passing the yield point, the stress values decrease continuously toward a steady-state

level representing the flow stress. As discussed in detail in Ref. [26], there is a strong correlation between this parameter and the plastic deformation mechanisms of nanostructured metals. To avoid the effect of fluctuations on the results, here, the average of the stress values in the strain range of 0.2–0.4 was considered as the flow stress, which is a common procedure in the literature [23]. It is noted that in this deformation stage, plastic flow took place in all Ta samples examined in Fig. 3.

As illustrated in Fig. 3, the values of yield strength and maximum stress reduce as the grain size decreases. Figures 4 and 5 show the variations of elastic modulus and flow stress with the average grain size of the Ta sample, respectively. As seen, the elastic modulus shows an inverse correlation with the GB density, and it decreases as the average grain size decreases (i.e., the number of GB atoms increases). As discussed by Li et al. [26], this is attributed to the larger potential energy of atoms in GBs compared to those within the grains. As such, the contribution of GB atoms to elastic resistance is lower than the atoms within the grains. Comparing the variation of flow stress with Ta grain size in the present study with that of the samples analyzed at 10 K by Huang et al. [23] (see Fig. 5), it is found that the breakdown in the Hall–Petch relationship occurs for larger grain-sized sample at 310 K. We plotted in Fig. 6 the flow stress against the inverse square root of the grain size at the strain of 0.05 for the samples with grain sizes smaller than 8 nm, in accordance with Pan et al. [21]. The linear trend of the fit curve demonstrates the grain-boundary-based plastic deformation mechanisms in fine-grained samples. Also, the flow stress values are

**Figure 1** Initial configuration of polycrystalline Ta sample with an average grain size of 8 nm. Atoms are colored based on the CNA method. Dark blue color denotes GBs, and yellow color indicates BCC Ta grain atoms.

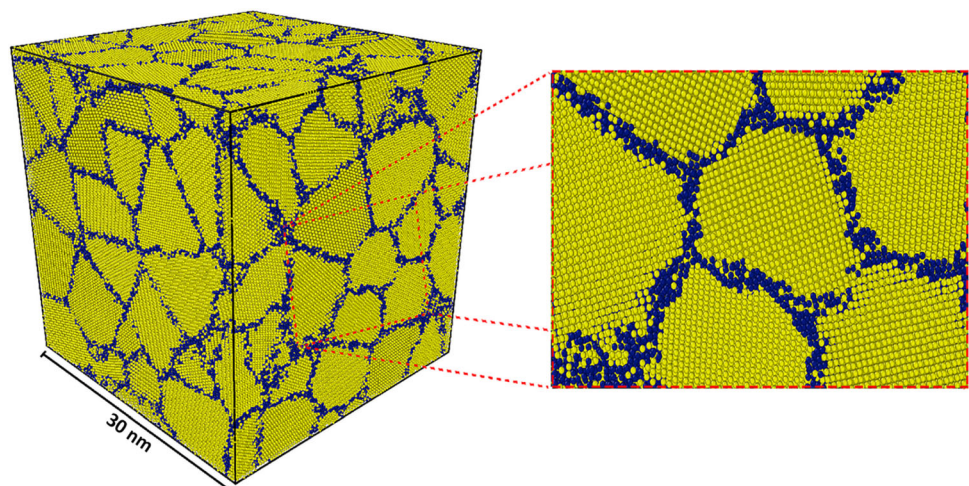
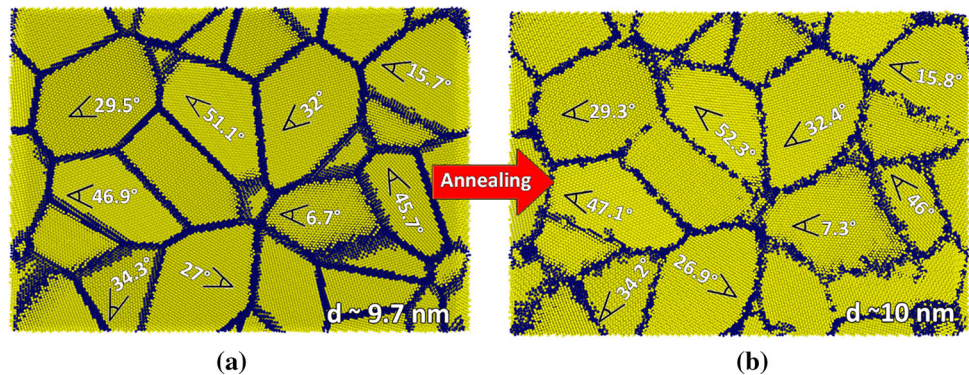


**Figure 2** Grain orientations and average grain size (denoted by  $d$ ) of the polycrystalline Ta sample **a** before and **b** after the hybrid annealing procedure. Atoms are colored based on the CNA method. Grain atoms are colored in yellow and GB atoms are distinguished by dark blue color.



considerably decreased at higher temperature conditions. In this context, the effect of temperature on the flow stress will be discussed in Sect. 3.4.

### Deformation of coarse-grained samples: twinning-based mechanisms

It has been demonstrated that the twinning-based plastic deformation is a favorable mechanism in nanostructured Ta at room temperature and high strain rates [22, 50, 51]. Accordingly, we wanted to check whether this mechanism is operative in our samples. This was achieved through inspection of the PTM analysis depicted in Fig. 7. In this figure, the letters D and T denote “dislocation” and “twin,” respectively. Also, the white lines in the zoomed regions of Figs. 7c–6f show the atomic arrangement at the two sides of the twin boundaries. Through analysis of the microstructural evolutions represented in Fig. 7, the following observations can be summarized:

- Twinning is the main mechanism governing the plastic deformation of the samples with an average grain size larger than 8 nm.
- With increasing strain, the density of twins increases. This feature is deduced by comparing parts b and f of Fig. 7.
- Triple junction (TJ) points are favorite sites for nucleation of twins (see T1, T3, and T4). This is attributed to the high stress level of TJs compared to the other regions of GBs, as demonstrated by Thomas et al. [52].
- By scanning the morphology of T1–T3, it is revealed that with increasing the strain level, old twins become thicker and thus twinned areas extend into the grains.

- High-angle grain boundaries can be considered as active sites for twin and dislocation nucleation as observed in Fig. 7a, e.
- Twin transmission and twin-GB interactions have not been observed in the studied samples up to the strain of 40%.

In this context, Jiang et al. [53] have experimentally analyzed the twin nucleation and growth over time in Ta samples under tensile loading. To facilitate comparison, we also monitored the twin nucleation and thickening for T3, as shown in Fig. 8a–e. In this case, the observed lateral growth reveals the coherent nature of twin boundaries. This issue agrees with the mentioned HRTEM observations provided in Fig. 8f–j showing the twin lamellae growth during the imposed strain. Such a twin growth phenomenon can successfully stabilize the twin structure within the grains in the deformation of polycrystalline materials.

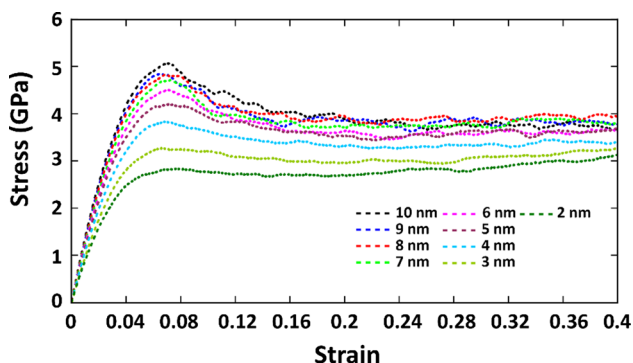
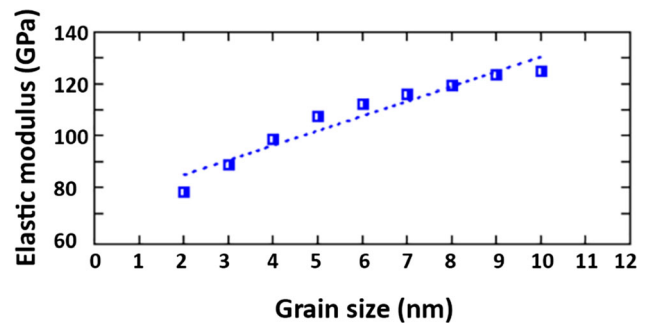
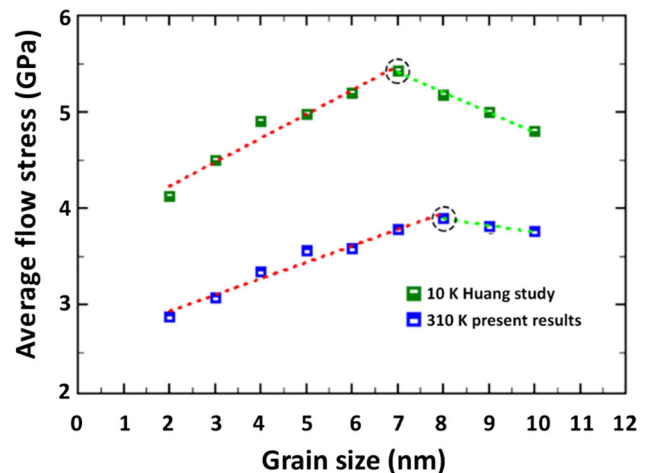
As mentioned before, the discussed twin nucleation and growth processes are not unique for the sample with 8 nm grain size. Similarly, the high-angle GBs and TJ points are favorable sites for twin nucleation in the samples with 9 and 10 nm grain sizes. To have quantitative evidence of the twin nucleation and growth stages for all of the coarse-grained samples, we compared their fraction of twin atoms with respect to all atoms at various strains. As illustrated in Fig. 9a, decreasing the grain size limits twin thickening during the deformation, which leads to the reduction of the twin-atom density [54]. Generally speaking, considering the small values of strain in the present work, a low density of twins would be expected to appear in the coarse-grained models. Therefore, no twin–twin interactions were detected in these samples. To shed more light on the twin growth mechanisms, we also calculated the density of twin partial dislocations,  $1/6 \langle 111 \rangle$ , for the

**Table 1** Mechanical properties of the Ta sample in the current study compared to the data given in the literature

Study	Assessment method	Yield strength (GPa)	Elastic modulus (GPa)	Maximum stress (GPa)	Flow stress (GPa)
Huang [23]	MD (EAM)	2.2	110.0	5.4	4.15
Present work	MD (ADP)	2.4	116.2	5.3	4.53

sample with an average grain size of 8 nm. As thoroughly discussed in the literature [55–57], the slip of mentioned dislocations at the twin tip results in the twin growth within the grains. As seen in Fig. 9b, there is a direct correlation between the twin partial dislocation line length and the imposed strain level. This finding has a good agreement with the fraction of twin atoms shown in Fig. 9a. In summary, it was deduced that twin partial dislocations play a significant role in the twin growth phenomenon in nanostructured tantalum.

As observed in Fig. 7, GBs are the main sources of dislocation emission. This phenomenon is probed in more detail in Fig. 10 using the DXA analysis method. While most of the grains are free from dislocations, our simulations provide direct evidence for the appearance of dislocations in the GB regions in all strain levels. With increasing strain, dislocation emission from GBs to the grain interiors is promoted. The mentioned dislocations are highlighted by red dashed circles in Fig. 10. Referring to the literature [58–60], GBs are regions with high energy, stress concentration, and microstrains. Accordingly, dislocations need lower stress values to be nucleated from these sites. Our findings can be well supported by analyzing the stress distribution pattern illustrated in Fig. 10f. The von Mises stress map in the strain of 0.1 shows that GBs experience more stress levels than

**Figure 3** Stress–strain diagram of polycrystalline Ta samples with various grain sizes under tension at 310 K.**Figure 4** Dependence of the elastic modulus of polycrystalline Ta on the average grain size at 310 K.**Figure 5** Comparison of the obtained flow stress for the polycrystalline Ta samples at 310 K with those reported by Huang et al. at 10 K.

grain interiors. Also, as we expected, stress is much more pronounced in the crystalline defects, namely twins and dislocations, compared to the perfect crystal parts. In summary, we found that for the sample with an average grain size of 8 nm, the main plastic deformation mechanisms are twinning and dislocation slip. Since the governing mechanisms are similar up to the breakdown point, the mentioned findings can be generalized to the samples with average grain size larger than 8 nm (see Fig. 5). It is worthy to note that although the dislocation–GB



interaction is an important phenomenon in such nanomaterials, no dislocation transmission was observed from one grain to the others in the present study. Additionally, we found that the perfect dislocations were stopped by GBs during the slip process. Consequently, it was deduced that GB regions act as a source/obstacle for the dislocation nucleation/slip for the coarse-grained Ta samples.

Considering the role of twins and dislocations on the mechanical response of these samples, it seems that changing the grain size would affect the proposed mechanism underlying their plastic deformation. To have a quantitative tool supporting this idea, the dislocation density and GB atoms fraction were obtained using DXA analysis for the samples with different grain sizes ranging from 2 to 10 nm. Figure 11a displays the calculated dislocation density for the introduced samples at 310 K. The dislocation density is defined as the total dislocation length per unit volume of the simulation box, ignoring the contribution of GB dislocations. As depicted in this figure, decreasing the grain size would lead to the reduction of dislocation density. Especially for the sample with a 2 nm average grain size, the dislocation density is much lower compared to the other cases, demonstrating that a different deformation mechanism governs its plastic deformation. On the other hand, as illustrated in Fig. 11b, there is an inverse correlation between the grain size and the

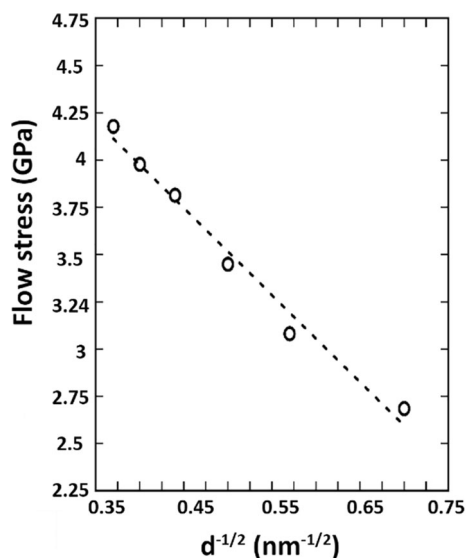


**Figure 6** Flow stress versus the inverse square root of the grain size,  $d$ , at a strain of 0.05 for the samples with grain sizes smaller than 8 nm.

fraction of GB atoms. Accordingly, it was concluded that GB-based mechanisms dominate the plastic deformation of Ta samples with smaller grain sizes.

### Deformation of fine-grained samples: grain-boundary-based mechanisms

The plastic deformation of polycrystalline Ta comprising small grains has been investigated previously in several studies. Tang et al. [24] studied the microstructural evolution of polycrystalline Ta with an average grain size of 5 nm under compressive loading conditions. It was revealed that the grain boundary rotation and grain elongation in the direction perpendicular to the imposed loading are the main plastic mechanisms in this case study. Employing MD simulation, Pan et al. [21] followed the motion of atoms for a strain of 0.15 compared to their initial configuration for a polycrystalline Ta sample with an average grain size of 6.5 nm. They successfully detected grain rotation and GB sliding utilizing the displacement vector map. Grain boundary motion was also reported by Huang et al. [23] in a polycrystalline Ta sample with 3 nm grain size during uniaxial tensile loading. Therefore, it seems that the best method to characterize the GB-dependent deformation mechanisms would be probing the atomic motion in the grains at different strain levels. As such, we inspected the movement of GB atoms for the sample with 4 nm grain size upon increasing the strain level from 0.1 to 0.4, as depicted in Fig. 12. In this figure, blue and red arrows indicate the movement direction of GB and interior atoms, respectively. Additionally, small black arrows in the red dashed boxes represent the atomic displacement vector of each atom.

The first mechanism detected in parts (a) and (b) of this figure is the grain elongation in the tensile direction, which is observed in the yellow grains. As disclosed in grains G1 and G2, it is ascribed to the GB motion arising from the atomic movements inside these grains. In addition, in several grains marked in red color (e.g., grain G3 in Fig. 12c), grain-size reduction perpendicular to the loading direction is found. Additionally, as thoroughly discussed in the literature, when a polycrystalline structure is under mechanical loading, grain boundaries may be impeded by the triple junctions leading to the bending of the entire boundary [61]. This issue would manifest itself for the orange grain shown in Fig. 12c. As seen,



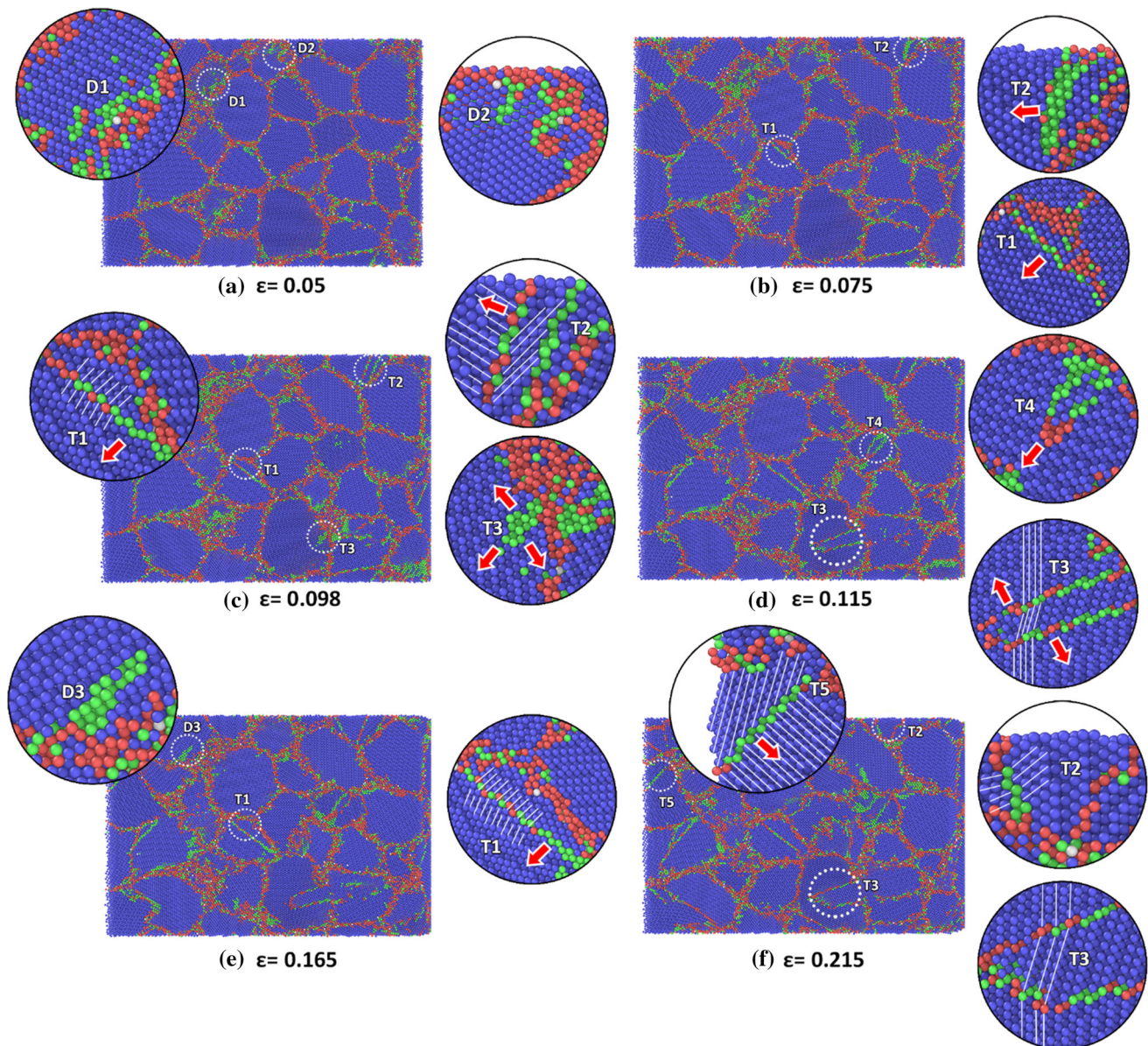


**Figure 7** PTM analysis results for the polycrystalline sample with an average grain size of 8 nm: **a–f** Detected twins and dislocations during tension. Blue color denotes BCC Ta grains, and green/red colors indicate GB atoms.

due to the GB migration, this grain would be bounded by the curved boundaries, as illustrated in Fig. 12d. Grain rotation is another GB-based phenomenon during tension for the introduced polycrystalline samples. It occurs when sliding of GBs in the opposite direction leads to the grain shear and, thus, grain rotation. Considering the data reported in Fig. 12, grain rotation was observed only in two grains (G4 and G5).

Consequently, it was concluded that GB sliding and migration are more dominant mechanisms than grain rotation during the deformation of small grain-

sized tantalum samples. It is worth mentioning that grain rotation causes strain hardening in metals [50]. As such, since no sign of strain hardening was observed in our stress–strain curves (see Fig. 3), we would not expect significant grain rotation in these case studies. To provide a picture of how the grain rotation influences the plastic deformation of small grain-sized polycrystalline metals, Wang et al. [62] studied a nanocrystalline platinum microstructure under tension using HRTEM. They found that increasing the dislocation length enhances the misorientation angle in these regions, which is the

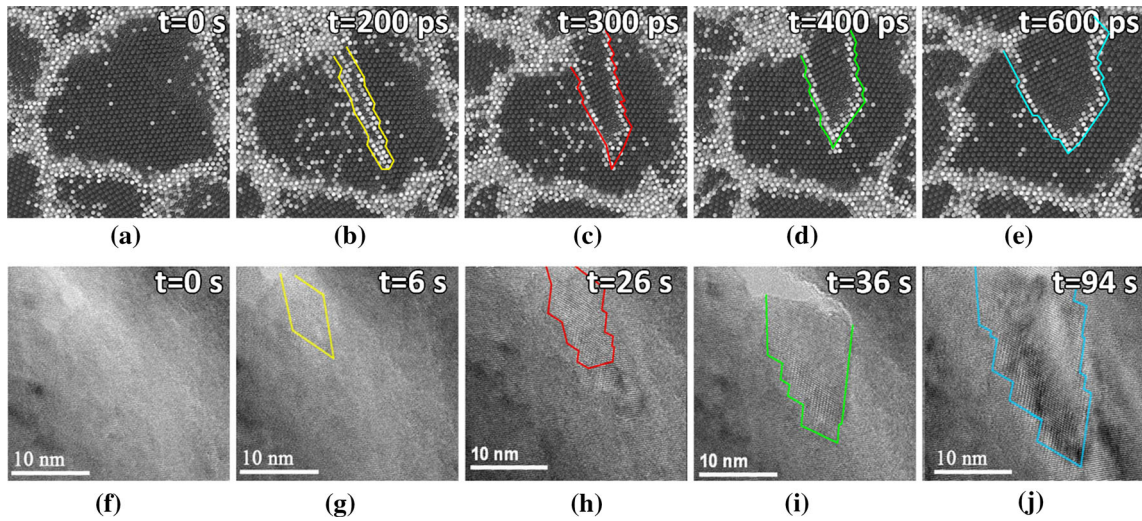
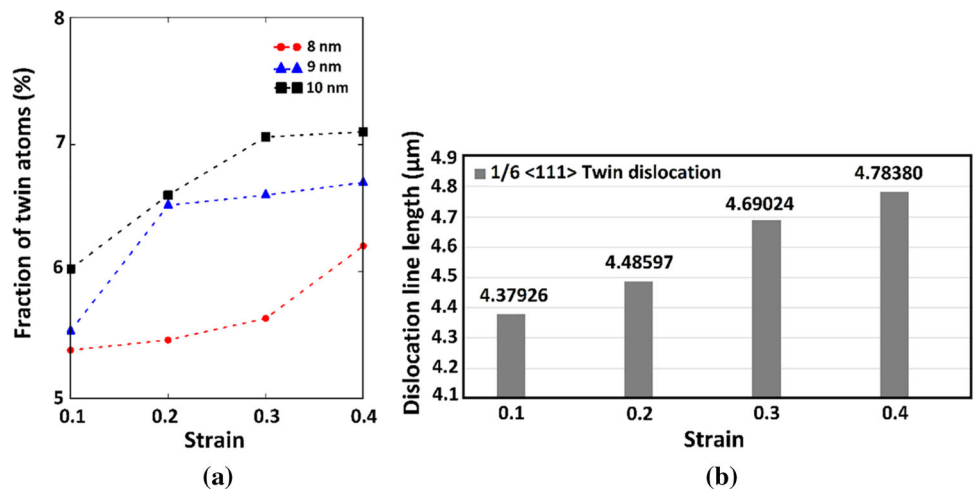


**Figure 8** Twin growth over time: **a–e** The present simulation data, **f–j** HRTEM analysis by Jiang et al. [53], reproduced with the permission of Elsevier. The atoms in figures **a–e** are colored by the CSP method. The dark atoms represent grain areas, and light atoms show GB and twin regions.

**Figure 9** Quantitative analysis of the twins in the coarse-grained samples: **a** Fraction of twin boundary atoms with respect to all atoms. **b** Twin dislocation line length of the sample with 8 nm grain size at different strains.



main driving force to rotate the grains. Therefore, considering the fact that for the discussed sample (i.e., the sample with 4 nm grain size), the dislocation density shows an increasing trend in the strain range of 0.3–0.4 (Fig. 11), the observed grain rotation at the higher levels of imposed strain is a reasonable phenomenon.

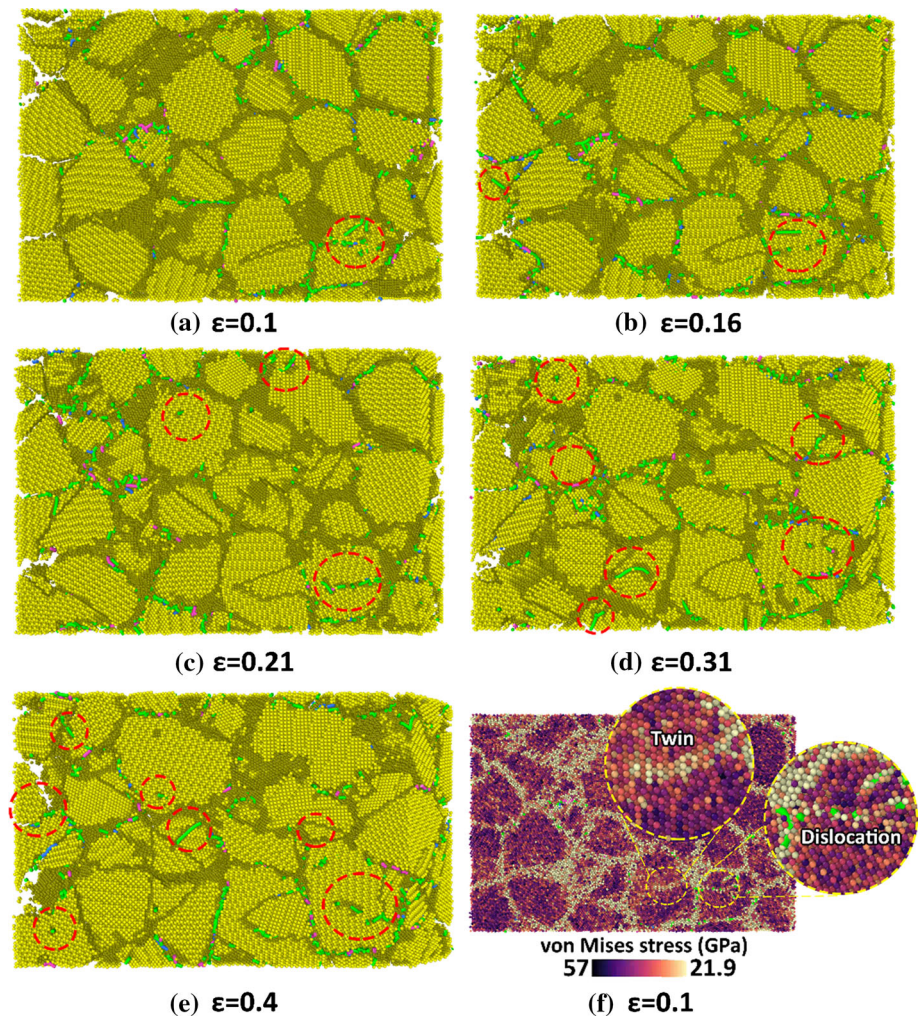
### Temperature-dependent Hall–Petch evolutions

In this part, the role of temperature on the mechanical properties and microstructural evolution of polycrystalline Ta samples is discussed. To this aim, the corresponding stress–strain curves are provided at

the temperature of 600 K, as shown in Fig. 13. Comparing the results with those of the samples that experienced the human-body temperature (see Fig. 3), one can notice that yield strength and maximum stress values decrease with the temperature rise. Such a declining trend was also found for the elastic modulus of the samples, as illustrated in Fig. 14. This is attributed to the enhanced atomic fluctuations at the elevated temperature conditions leading to increased interatomic distances, which is the main reason for the observed elastic modulus reduction. Flow stress is another crucial factor that would be affected by the temperature. Regarding this issue, Fig. 15 displays the variations of flow stress for the introduced polycrystalline tantalum samples



**Figure 10** DXA results for the polycrystalline sample with an average grain size of 8 nm: **a–e** Representation of the dislocation emission from the GB areas, **f** von Mises stress map at the strain of 0.1. In this figure, yellow atoms show grains, dark yellow atoms reveal GBs, and green color represents the dislocation lines.



analyzed at different temperatures of 10, 310, and 600 K. The results show the strong temperature dependence of the Hall–Petch breakdown threshold for Ta samples. As seen, with increasing the temperature, the discussed GB-based mechanisms are activated for samples with larger grain size.

Zhang et al. reported a similar behavior for high-entropy alloys upon increasing the temperature from 10 to 600 K [63]. They attributed this phenomenon to the limitation of dislocation glide at low temperatures due to increased frictional stress in these conditions. As Zhao et al. [64] have thoroughly discussed, GB migration and grain rotation play a significant role in the microscopic plastic deformation mechanisms at high-temperature processes. Overall, these phenomena reduce the flow stress making the polycrystalline

materials exhibit the inverse Hall–Petch effect in larger grain-sized samples.

To shed more light on this issue, GB movements have been atomistically probed for the sample with 8 nm grain size at various temperatures (Fig. 16). It should be pointed out that at 310 K, the sample has the critical grain size of the Hall–Petch relationship. However, as depicted in Fig. 15, due to the change of the breakdown point, this sample experiences the inverse Hall–Petch effect at 600 K. In Fig. 16, the blue and red maps represent the GB locations of the sample at 310 and 600 K, respectively. To facilitate better comparison, the microstructural evolutions have been monitored at the same levels of imposed tensile strain. In this figure, black arrows show the movement direction of red GBs compared to their

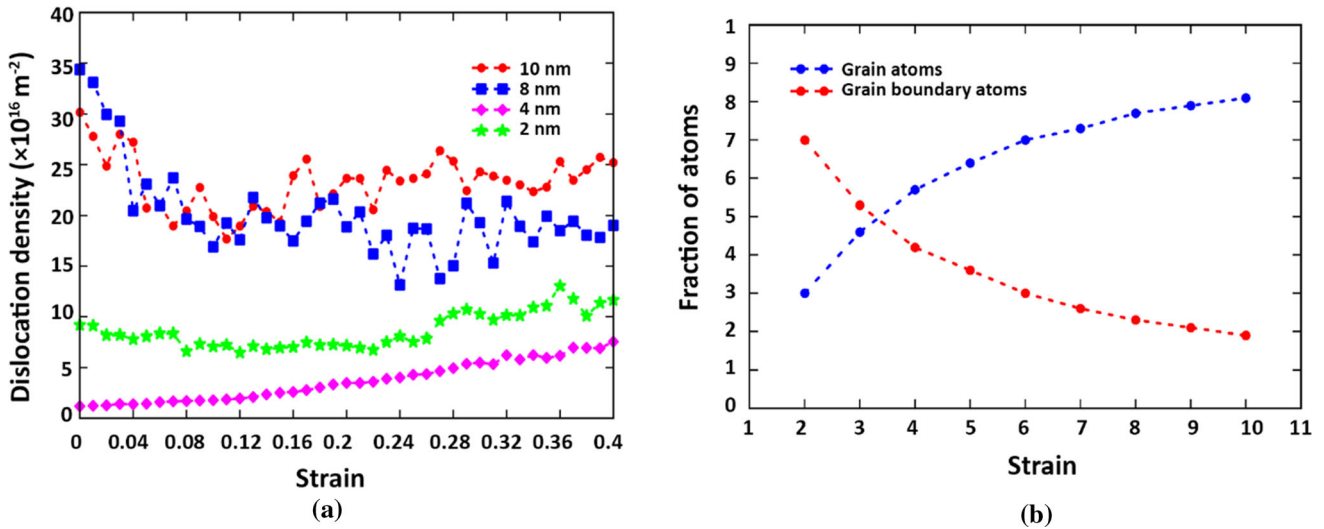


**Figure 11** Quantitative analysis of structural defects for polycrystalline Ta samples with various average grain sizes: dependence of **a** dislocation density and **b** fraction of GB atoms on the strain.

state in the previous strain. As seen, in the strain range of 0.15–0.25, higher amounts of GB migration can be observed in grains G1–G3 and G5 of the sample at 600 K. Thereafter, as the strain increases to the range of 0.3–0.4, the grain boundary movement increases in all grains (see Fig. 16d–f). Accordingly, it was concluded that the plastic deformation mechanisms in the sample with an average grain size of 8 nm change from dislocation slip and twinning at 310 K to GB-based mechanisms at 600 K.

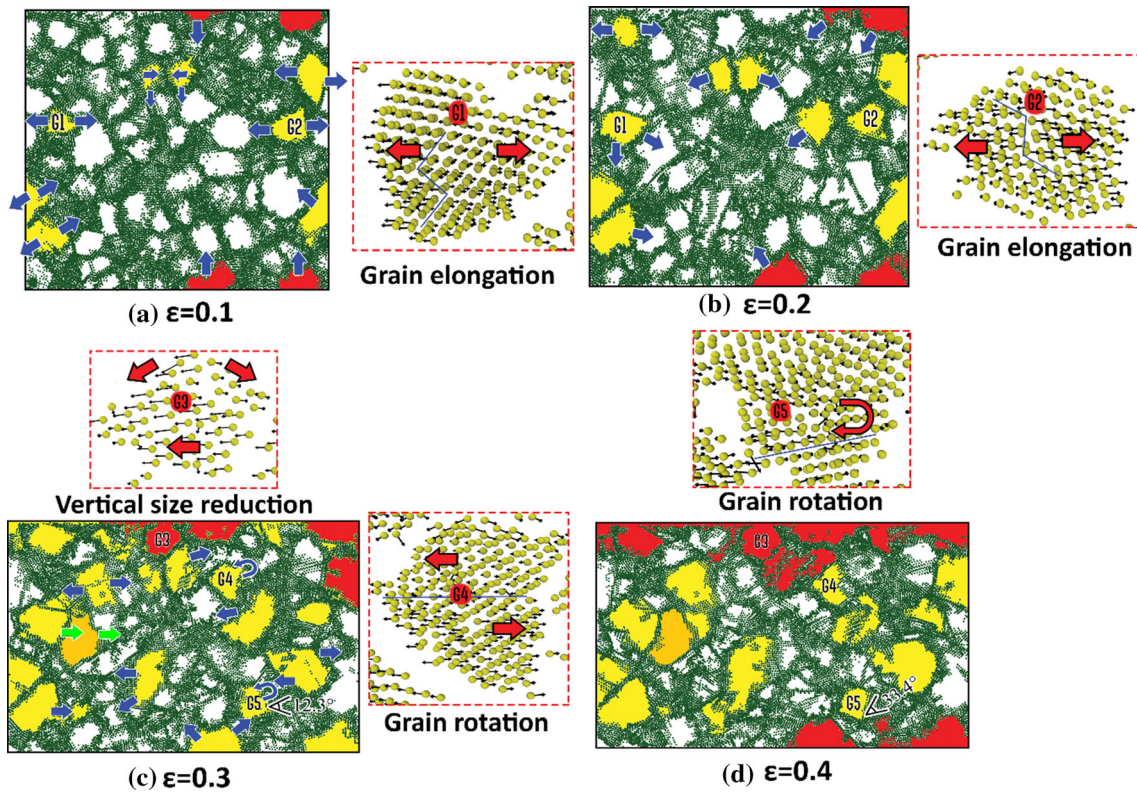
It is worthy of mention that in addition to the coarse-grained samples, the plastic deformation of ultra-fine-grained models is also influenced by temperature. As shown in Fig. 13, the strain-hardening phenomenon is observed for the sample with the smallest grain size at high values of imposed strain. This issue is attributed to the forest-hardening at high strain levels, which is a direct result of partial dislocation interactions and dislocation multi-junctions [46, 65–67]. To provide a better understanding of this issue, we compared the line length of partial and perfect dislocations for the sample with 2 nm grain size at the temperatures of 310 and 600 K. As depicted in Fig. 17, the density of partial dislocations increases as the temperature rises. As discussed by Du et al. [68], this phenomenon is associated with the reduction of the stress required for dislocation nucleation from the GB areas at higher temperature conditions. Therefore, in the case of ultra-fine-grained

Ta structures, a large number of dislocations can be formed within the samples due to the presence of a high density of GBs and thermal energy activation, leading to the observed strain hardening, especially at elevated temperatures.

## Summary

In this paper, a series of MD simulations were carried out to characterize the tensile mechanical properties and plastic deformation behavior of polycrystalline Ta implants. To this aim, at first, several Ta samples with an average grain size in the range of 2–10 nm were systematically examined at the human-body temperature (i.e., 310 K). The results demonstrated that the elastic modulus and yield strength of the samples decrease monotonically if the grain size is reduced. This behavior was attributed to the increase of GB density, which weakens the elastic resistance of the whole sample. Furthermore, the critical grain size of polycrystalline tantalum samples resulting in the maximum strength was determined for this temperature. It was concluded that the sample with an average grain size of 8 nm could be considered as the case with the best mechanical performance. To comprehensively address this issue, using various crystal structure analysis tools provided by the OVITO software, we probed the microstructural evolution in

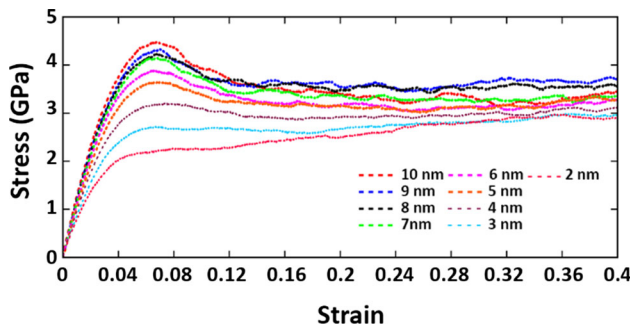




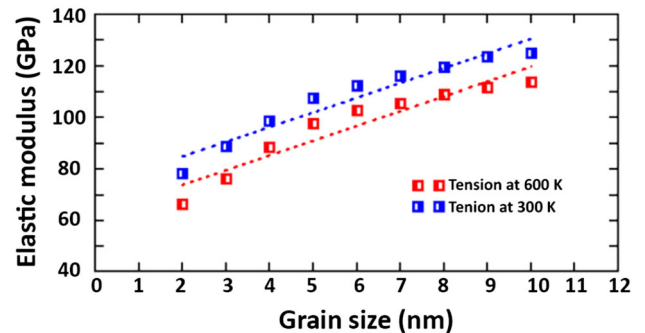
**Figure 12** GB-based microstructural evolution during tension for the polycrystalline sample with an average grain size of 4 nm at different strains: **a**  $\epsilon = 0.1$ , **b**  $\epsilon = 0.2$ , **c**  $\epsilon = 0.3$ , and **d**  $\epsilon = 0.4$ . The green atoms distinguished by the CNA analysis represent GB areas.

the samples with an average grain size of 8 and 4 nm. It was revealed that in the former sample, the plastic deformation occurs by twinning formation and dislocation slip. In contrast, GB-based phenomena such as sliding, rotation, and migration are responsible for the deformation of fine-grained samples. Moreover, to explore the temperature effects on the GB-based mechanisms, we further proceeded to simulate the

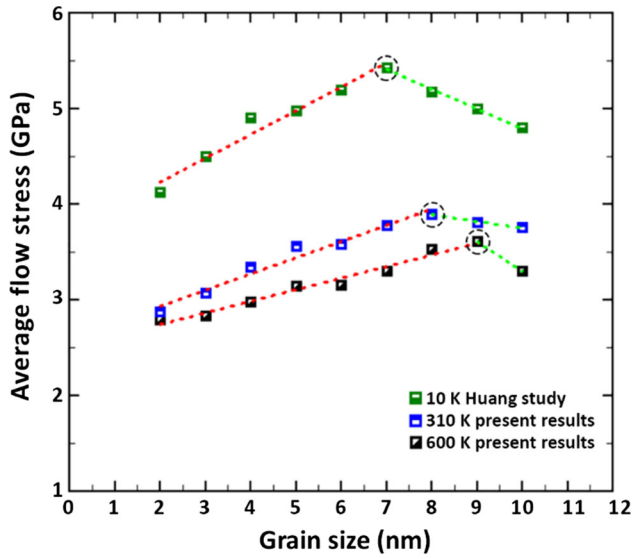
sample with an average grain size of 8 nm at 600 K. Comparing the results with those of the sample at the human-body temperature, it was deduced that at higher temperature conditions, GB migration and grain rotation play a significant role in the microscopic plasticity induced within the nanostructured polycrystalline Ta samples. This phenomenon would manifest itself as a shift observed in the breakpoint of



**Figure 13** Stress–strain diagram of polycrystalline Ta samples with various grain sizes under tension at 600 K.



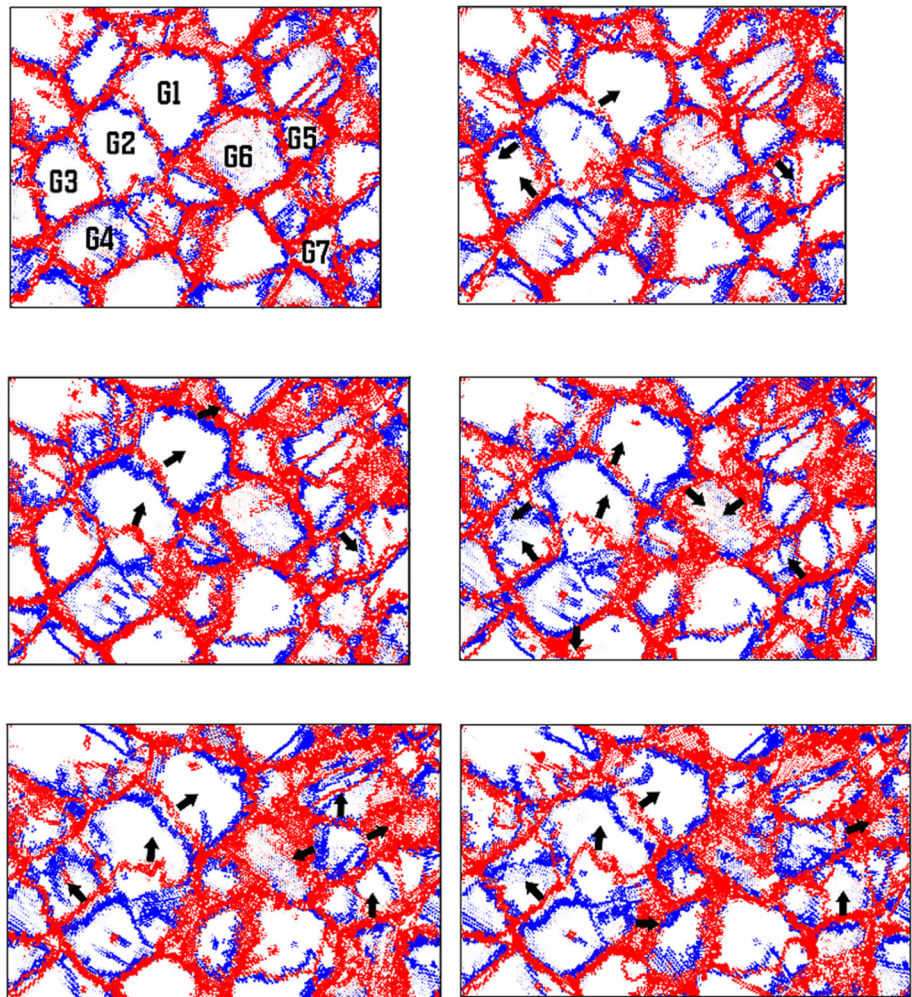
**Figure 14** Grain-size dependence of the elastic modulus for the polycrystalline Ta samples at two temperatures.



**Figure 15** Shift of the Hall–Petch breakdown for the polycrystalline Ta samples at various temperatures.

the Hall–Petch relationship from 8 to 9 nm. As such, it was concluded that the governing plastic deformation mechanisms in the sample with 8 nm grain size change from dislocation slip and twinning at 310 K to GB-based mechanisms at 600 K. We believe that the framework developed here could be helpful not only to explore the governing plastic deformation mechanisms of nanostructured metals, but also to tailor the mechanical performance of polycrystalline Ta samples as medical implants.

**Figure 16** Evolution of GBs of the Ta sample with an average grain size of 8 nm during tension at the temperatures of 310 and 600 K at different strains: **a**  $\epsilon = 0.15$ , **b**  $\epsilon = 0.2$ , **c**  $\epsilon = 0.25$ , **d**  $\epsilon = 0.3$ , **e**  $\epsilon = 0.35$ , and **f**  $\epsilon = 0.4$ . Blue and red colors denote GBs at 310 and 600 K, respectively.





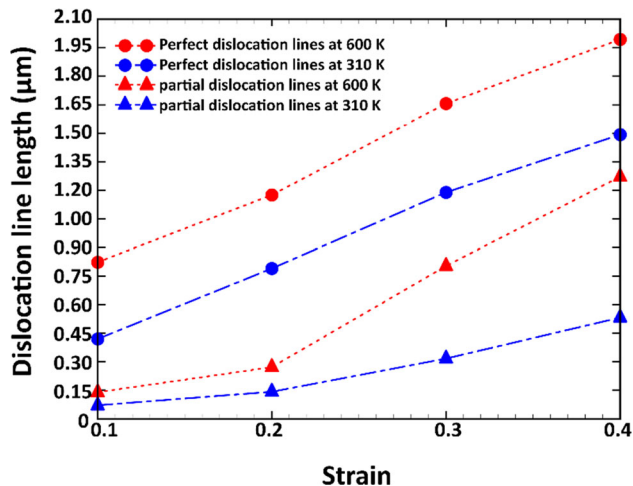


**Figure 17** Comparison of the dislocation line length of the sample with 2 nm grain size at 310 and 600 K.

## Acknowledgements

Simulations were performed at the High Performance Cluster Elwetritsch (RHRK, TU Kaiserslautern, Germany).

## Funding

Open Access funding enabled and organized by Projekt DEAL. The authors acknowledge support by the Deutsche Forschungsgemeinschaft (DFG, German Research Foundation)—Project Number 441110175—UR 32/28–1.

## Declarations

**Conflict of interests** The authors declare that they have no conflict of interest.

**Open Access** This article is licensed under a Creative Commons Attribution 4.0 International License, which permits use, sharing, adaptation, distribution and reproduction in any medium or format, as long as you give appropriate credit to the original author(s) and the source, provide a link to the Creative Commons licence, and indicate if changes were made. The images or other third party material in this article are included in the article's Creative Commons licence, unless indicated otherwise in a credit line to the material. If material is not included in the article's Creative Commons licence and your intended use is not permitted by statutory regulation or exceeds the

permitted use, you will need to obtain permission directly from the copyright holder. To view a copy of this licence, visit <http://creativecommons.org/licenses/by/4.0/>.

## References

- [1] Bandyopadhyay A, Mitra I, Shivaram A, Dasgupta N, Bose S (2019) Direct comparison of additively manufactured porous titanium and tantalum implants towards in vivo osseointegration. *Addit Manuf* 28:259–266
- [2] Sakaguchi RL, Powers JM (2012) *Craig's restorative dental materials-e-book*. Elsevier Health Sciences, Amsterdam
- [3] Paganias CG, Tsakotos GA, Koutsostahis SD, Macherasm GA (2014) The process of porous tantalum implants osseous integration a review. *Current Res Med* 5:63–72
- [4] Soro N, Attar H, Brodie E, Veidt M, Molotnikov A, Dargusch MS (2019) Evaluation of the mechanical compatibility of additively manufactured porous Ti–25Ta alloy for load-bearing implant applications. *J Mech Behav Biomed Mater* 97:149–158
- [5] Shi L-Y, Wang A, Zang F-Z, Wang J-X, Pan X-W, Chen H-J (2017) Tantalum-coated pedicle screws enhance implant integration. *Colloids Surfaces B Biointerfaces* 160:22–32
- [6] Sagherian BH, Claridge RJ (2019) The use of tantalum metal in foot and ankle surgery. *Orthop Clin North Am* 50:119–129
- [7] Misch CE (2004) *Dental implant prosthetics-E-book*. Elsevier Health Sciences, Amsterdam
- [8] Mi ZR, Shuib S, Hassan A, Shorki A, Ibrahim M (2007) Problem of stress shielding and improvement to the hip implant designs: a review. *J Med Sci* 7:460–467
- [9] Balla VK, Bodhak S, Bose S, Bandyopadhyay A (2010) Porous tantalum structures for bone implants: fabrication, mechanical and in vitro biological properties. *Acta Biomater* 6:3349–3359
- [10] Balla VK, Bose S, Davies NM, Bandyopadhyay A (2010) Tantalum—a bioactive metal for implants. *JOM J Mineral Metals Mater Soc* 62:61–64
- [11] Villapún VM, Dover LG, Cross A, González S (2016) Antibacterial metallic touch surfaces. *Materials* 9:736
- [12] Hsieh JH, Yeh TH, Li C, Chiu CH, Huang CT (2013) Antibacterial properties of TaN–(Ag, Cu) nanocomposite thin films. *Vacuum* 87:160–163
- [13] Sharma A, Chaudhari BK, Shrestha B, Suwal P, Parajuli PK, Singh R, Niraula SR (2019) Knowledge and perception about dental implants among undergraduate dental students. *BDJ open* 5:1–5

- [14] Frost HM (1994) Wolff's Law and bone's structural adaptations to mechanical usage: an overview for clinicians. *Angle Orthod* 64:175–188
- [15] Zhao X, Lu C, Tieu AK, Zhan L, Pei L, Huang M (2018) Deformation mechanisms and slip-twin interactions in nanotwinned body-centered cubic iron by molecular dynamics simulations. *Comput Mater Sci* 147:34–48
- [16] Chowdhury P, Sehitoglu H (2018) Atomistic energetics and critical twinning stress prediction in face and body centered cubic metals: recent progress. *J Eng Mater Technol* 140:020801
- [17] Ruestes CJ, Bringa EM, Stukowski A, Rodrigue Znieva JF, Tang Y, Meyers MA (2014) Plastic deformation of a porous bcc metal containing nanometer sized voids. *Comput Mater Sci* 88:92–102
- [18] Wang ZQ, Beyerlein IJ (2011) An atomistically-informed dislocation dynamics model for the plastic anisotropy and tension–compression asymmetry of BCC metals. *Int J Plast* 27:1471–1484
- [19] Hahn EN, Meyers MA (2015) Grain-size dependent mechanical behavior of nanocrystalline metals. *Mater Sci Eng, A* 646:101–134
- [20] Weinberger CR, Tucker GJ (2016) Multiscale materials modeling for nanomechanics. Springer, Cham
- [21] Pan Z, Li Y, Wei Q (2008) Tensile properties of nanocrystalline tantalum from molecular dynamics simulations. *Acta Mater* 56:3470–3480
- [22] Sun H, Kumar A, Singh CV (2019) Deformation behavior of BCC tantalum nanolayered composites with modulated layer thicknesses. *Mater Sci Eng A* 761:138037
- [23] Huang C, Peng X, Zhao Y, Weng S, Yang B, Fu T (2018) Flow strength limit of nanocrystalline tantalum predicted with molecular dynamics simulations. *Mater Sci Eng A* 738:1–9
- [24] Tang Y, Bringa EM, Meyers MA (2013) Inverse Hall–Petch relationship in nanocrystalline tantalum. *Mater Sci Eng A* 580:414–426
- [25] Smith L, Zimmerman JA, Hale LM, Farkas D (2014) Molecular dynamics study of deformation and fracture in a tantalum nano-crystalline thin film. *Modell Simul Mater Sci Eng* 22:045010
- [26] Li J, Lu B, Zhou H, Tian C, Xian Y, Hu G, Xia R (2019) Molecular dynamics simulation of mechanical properties of nanocrystalline platinum: grain-size and temperature effects. *Phys Lett A* 383:1922–1928
- [27] Ono N, Nowak R, Miura S (2004) Effect of deformation temperature on Hall–Petch relationship registered for polycrystalline magnesium. *Mater Lett* 58:39–43
- [28] Naik SN, Walley SM (2020) The Hall–Petch and inverse Hall–Petch relations and the hardness of nanocrystalline metals. *J Mater Sci* 55:2661–2681. <https://doi.org/10.1007/s10853-019-04160-w>
- [29] Rycroft CH (2009) VORO++: a three-dimensional Voronoi cell library in C++, *Chaos: an interdisciplinary*. *J Nonlinear Sci* 19:041111
- [30] Falco S, Jiang J, Cola FD, Petrinic N (2017) Generation of 3D polycrystalline microstructures with a conditioned Laguerre–Voronoi tessellation technique. *Comput Mater Sci* 136:20–28
- [31] Plimpton S (1995) Fast parallel algorithms for short-range molecular dynamics. *J Comput Phys* 117:1–19
- [32] Purja Pun GP, Darling KA, Kecskes LJ, Mishin Y (2015) Angular-dependent interatomic potential for the Cu–Ta system and its application to structural stability of nano-crystalline alloys. *Acta Mater* 100:377–391
- [33] Kale C, Srinivasan S, Hornbuckle BC, Koju RK, Darling K, Mishin Y, Solanki KN (2020) An experimental and modeling investigation of tensile creep resistance of a stable nanocrystalline alloy. *Acta Mater* 199:141–154
- [34] Chen J, Tschopp MA, Dongare AM (2018) Role of nanoscale Cu/Ta interfaces on the shock compression and spall failure of nanocrystalline Cu/Ta systems at the atomic scales. *J Mater Sci* 53:5745–5765. <https://doi.org/10.1007/s10853-017-1879-7>
- [35] Chen J, Mathaudhu SN, Thadhani N, Dongare AM (2020) Unraveling the role of interfaces on the spall failure of Cu/Ta multilayered systems. *Sci Rep* 10:208
- [36] Darling KA, Srinivasan S, Koju RK, Hornbuckle BC, Smeltzer J, Mishin Y, Solanki KN (2021) Stress-driven grain refinement in a microstructurally stable nanocrystalline binary alloy. *Scripta Mater* 191:185–190
- [37] Gunkelmann N, Bringa EM, Kang K, Ackland GJ, Ruestes CJ, Urbassek HM (2012) Polycrystalline iron under compression: plasticity and phase transitions. *Phys Rev B* 86:144111
- [38] Allen MP, Tildesley DJ (2017) Computer simulation of liquids. Oxford University Press, Oxford
- [39] Wei J, Feng B, Ishikawa R, Yokoi T, Matsunaga K, Shibata N, Ikuhara Y (2021) Direct imaging of atomistic grain boundary migration. *Nat Mater* 20:951–955
- [40] Dremov VV, Chirkov PV, Karavaev AV (2021) Molecular dynamics study of the effect of extended ingrain defects on grain growth kinetics in nanocrystalline copper. *Sci Rep* 11:934
- [41] Danilenko V, Bachurin D, Nazarov A (2018) Annealing-induced grain rotation in ultrafine-grained aluminum alloy. *Rev Adv Mater Sci* 55:69–77
- [42] Larsen PM, Schmidt S, Schiøtz J (2016) Robust structural identification via polyhedral template matching. *Modell Simul Mater Sci Eng* 24:055007



- [43] Fan H, Liu S, Deng C, Wu X, Cao L, Liu Q (2018) Quantitative analysis: How annealing temperature influences recrystallization texture and grain shape in tantalum. *Int J Refract Metal Hard Mater* 72:244–252
- [44] El Shawish S, Cizelj L (2016) Numerical investigation of grain misorientations at and close to the free surface of FCC polycrystalline metals. *Comput Mater Sci* 113:133–142
- [45] Ma Y, Zhang S, Xu Y, Liu X, Luo S-N (2020) Effects of temperature and grain size on deformation of polycrystalline copper–graphene nanolayered composites. *Phys Chem Chem Phys* 22:4741–4748
- [46] Alcalá J, Očenášek J, Varillas J, El-Awady JA, Wheeler JM, Michler J (2020) Statistics of dislocation avalanches in FCC and BCC metals: dislocation mechanisms and mean swept distances across microsample sizes and temperatures. *Sci Rep* 10:19024
- [47] Stukowski A (2009) Visualization and analysis of atomistic simulation data with OVITO—the open visualization tool. *Modell Simul Mater Sci Eng* 18:015012
- [48] Stukowski A, Albe K (2010) Extracting dislocations and non-dislocation crystal defects from atomistic simulation data. *Modell Simul Mater Sci Eng* 18:085001
- [49] Kelchner CL, Plimpton SJ, Hamilton JC (1998) Dislocation nucleation and defect structure during surface indentation. *Phys Rev B* 58:11085–11088
- [50] Fang T-H, Huang C-C, Chiang T-C (2016) Effects of grain size and temperature on mechanical response of nanocrystalline copper. *Mater Sci Eng, A* 671:1–6
- [51] Huang C, Peng X, Fu T, Chen X, Xiang H, Li Q, Hu N (2017) Molecular dynamics simulation of BCC Ta with coherent twin boundaries under nanoindentation. *Mater Sci Eng, A* 700:609–616
- [52] Thomas SL, Chen K, Han J, Purohit PK, Srolovitz DJ (2017) Reconciling grain growth and shear-coupled grain boundary migration. *Nat Commun* 8:1764
- [53] Jiang B, Tu A, Wang H, Duan H, He S, Ye H, Du K (2018) Direct observation of deformation twinning under stress gradient in body-centered cubic metals. *Acta Mater* 155:56–68
- [54] Chen J, Dong F-T, Liu Z-Y, Wang G-D (2021) Grain size dependence of twinning behaviors and resultant cryogenic impact toughness in high manganese austenitic steel. *J Market Res* 10:175–187
- [55] Feng Y-X, Shang J-X, Qin S-J, Lu G-H, Chen Y (2018) Twin and dislocation mechanisms in tensile W single crystal with temperature change: a molecular dynamics study. *Phys Chem Chem Phys* 20:17727–17738
- [56] Wang J, Zeng Z, Wen M, Wang Q, Chen D, Zhang Y, Wang P, Wang H, Zhang Z, Mao SX, Zhu T (2020) Anti-twinning in nanoscale tungsten. *Sci Adv.* <https://doi.org/10.1126/sciadv.aay2792>
- [57] Altenbach H, Brünig M, Kowalewski Z (2020) *Plasticity, Damage and fracture in advanced materials.* Springer, Cham
- [58] Zhang Z, Ódor É, Farkas D, Jóni B, Ribárik G, Tichy G, Nandam S-H, Ivanisenko J, Preuss M, Ungár T (2020) Dislocations in Grain Boundary Regions: the origin of heterogeneous microstrains in nanocrystalline materials. *Metall Mater Trans A* 51:513–530
- [59] Li XY, Jin ZH, Zhou X, Lu K (2020) Constrained minimal-interface structures in polycrystalline copper with extremely fine grains. *Science* 370:831–836
- [60] Shibuta Y, Sakane S, Miyoshi E, Okita S, Takaki T, Ohno M (2017) Heterogeneity in homogeneous nucleation from billion-atom molecular dynamics simulation of solidification of pure metal. *Nat Commun* 8:10
- [61] Zhang L, Shibuta Y, Huang X, Lu C, Liu M (2019) Grain boundary induced deformation mechanisms in nanocrystalline Al by molecular dynamics simulation: From interatomic potential perspective. *Comput Mater Sci* 156:421–433
- [62] Wang L, Teng J, Liu P, Hirata A, Ma E, Zhang Z, Chen M, Han X (2014) Grain rotation mediated by grain boundary dislocations in nanocrystalline platinum. *Nat Commun* 5:4402
- [63] Zhang L, Shibuta Y (2020) Inverse Hall–Petch relationship of high-entropy alloy by atomistic simulation. *Mater Lett* 274:128024
- [64] Zhao Y, Chen Z, Long J, Yang T (2014) Influence of temperature on the inverse Hall–Petch effect in nanocrystalline materials: phase field crystal simulation. *Acta Metallurgica Sinica (English Letters)* 27:81–86
- [65] Bulatov VV, Hsiung LL, Tang M, Arsenlis A, Bartelt MC, Cai W, Florando JN, Hiratani M, Rhee M, Hommes G, Pierce TG, de la Rubia TD (2006) Dislocation multi-junctions and strain hardening. *Nature* 440:1174–1178
- [66] Yamakov V, Wolf D, Phillpot SR, Mukherjee AK, Gleiter H (2004) Deformation-mechanism map for nanocrystalline metals by molecular-dynamics simulation. *Nat Mater* 3:43–47
- [67] Fan H, Wang Q, El-Awady JA, Raabe D, Zaiser M (2021) Strain rate dependency of dislocation plasticity. *Nat Commun* 12:1845
- [68] Du J-P, Wang Y-J, Lo Y-C, Wan L, Ogata S (2016) Mechanism transition and strong temperature dependence of dislocation nucleation from grain boundaries: an accelerated molecular dynamics study. *Phys Rev B* 94:104110

**Publisher's Note** Springer Nature remains neutral with regard to jurisdictional claims in published maps and institutional affiliations.